ACS Infectious Diseases

pubs.acs.org/journal/aidcbc

Article

Serinc5 Restricts HIV Membrane Fusion by Altering Lipid Order and Heterogeneity in the Viral Membrane

Amanda E. Ward,* Daria Sokovikova, Melvin Neal Waxham, Frederick A. Heberle, Ilya Levental, Kandice R. Levental, Volker Kiessling, Judith M. White, and Lukas K. Tamm*

Cite This: *ACS Infect. Dis.* 2023, 9, 773−784

Read Online

ACCESS | Metrics & More | Article Recommendations | Supporting Information

ABSTRACT: The host restriction factor, Serinc5, incorporates into budding HIV particles and inhibits their infection by an incompletely understood mechanism. We have previously reported that Serinc5 but not its paralogue, Serinc2, blocks HIV cell entry by membrane fusion, specifically by inhibiting fusion pore formation and dilation. A body of work suggests that Serinc5 may alter the conformation and clustering of the HIV fusion protein, Env. To contribute an additional perspective to the developing model of Serinc5 restriction, we assessed Serinc2 and Serinc5's effects on HIV pseudoviral membranes. By measuring pseudoviral membrane thickness via cryo-electron microscopy and order via the fluorescent dye, FLIPPER-TR, Serinc5 was found to increase membrane heterogeneity, skewing the distribution toward a larger fraction of the viral membrane in an ordered phase. We also directly observed for the first time the coexistence of membrane domains within individual viral membrane envelopes. Using a total internal reflection fluorescence-based single particle fusion assay, we found that treatment of HIV pseudoviral particles with phosphatidylethanolamine (PE) rescued HIV pseudovirus fusion from restriction by Serinc5, which was accompanied by decreased membrane heterogeneity and order. This effect was specific for PE and did not depend on acyl chain length or saturation. Together, these data suggest that Serinc5 alters multiple interrelated properties of the viral membrane—lipid chain order, rigidity, line tension, and lateral pressure—which decrease the accessibility of fusion intermediates and disfavor completion of fusion. These biophysical insights into Serinc5 restriction of HIV infectivity could contribute to the development of novel antivirals that exploit the same weaknesses.

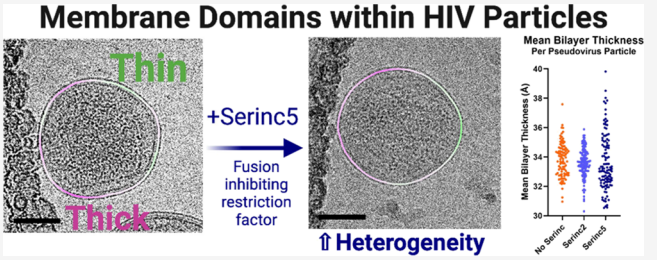

KEYWORDS: *lipid nanodomain, restriction factor, viral membrane fusion, HIV, Serinc5*

Serinc5 is a recently described host restriction factor that incorporates into budding HIV particles and inhibits infection at the cell entry step.[1,2] While it is known to inhibit multiple steps of membrane fusion—hemifusion, fusion pore opening, and fusion pore dilation[3,4]—the exact mechanism by which it does so remains uncertain. Many studies have focused on the interaction between Serinc5 and the HIV fusion protein, Env, demonstrating that Serinc5 alters Env conformation,[5,6] antibody binding,[4,7] and clustering.[8] However, alterations in Env cannot fully explain the observed fusion defects induced by Serinc5 incorporation. In current models of viral membrane fusion, progression through receptor binding, hemifusion, and early fusion pore formation is driven by rearrangements of the viral fusion protein and membrane deformation.[9,10] However, the penultimate step, fusion pore dilation, is driven by membrane tension and curvature.[11] Disruption of fusion pore dilation, as we previously observed with Serinc5-containing HIV pseudoviruses,[3] suggests that Serinc5 may alter fluid mechanical properties of the viral membrane. Increased viral membrane stiffness would require a larger input of energy to deform the membrane into highly curved intermediates like hemifusion stalks[12] and fusion pores.[13] Changing lipid biophysical properties of the viral membrane (often via cholesterol depletion) has been shown to reduce fusion of HIV and other enveloped viruses.[14−24]

While it has already been shown that Serinc5 does not change the overall lipid composition of the viral membrane,[25] membrane organization could be altered by other means, thereby affecting local concentrations of lipids. Model membranes of similar composition to the HIV membrane were shown to support liquid−liquid phase separation.[26−28] Specifically, areas enriched in saturated phospholipids, cholesterol, and sphingolipids form domains with a more ordered packing of lipid acyl chains that coexist with regions of unsaturated phospholipids, less cholesterol, and fewer

Received: September 22, 2022
Published: March 22, 2023

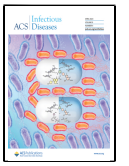

https://doi.org/10.1021/acsinfecdis.2c00478
ACS Infect. Dis. 2023, 9, 773−784

sphingolipids packed in a more disordered manner; these two phases are termed liquid-ordered (L_o) and liquid-disordered (L_d), respectively.[29] As a consequence of ordered packing, membranes in an L_o phase have different lateral pressure profiles and are several angstroms thicker than membranes in an L_d phase.[30] Lipid order and packing parameters can be reported by specific fluorescent membrane probes,[31−33] some of which are also suitable for imaging in cellular and viral membranes. More recently, heterogeneity of membrane thickness was directly observed by cryogenic electron microscopy (cryoEM) in model membranes composed of pure lipids as well as isolated plasma membrane vesicles.[34,35] Additionally, the host plasma membrane, from which the HIV viral membrane is derived, has an asymmetric lipid distribution, in which the outer leaflet is enriched in sphingomyelin (SM) and phosphatidylcholine (PC), while phosphatidylethanolamine (PE) and phosphatidylserine (PS) are actively sequestered on the inner leaflet. PE and PS are only present in the outer leaflet of the plasma membrane in times of cellular stress[36] but are detectable in the outer leaflet of the HIV envelope[26,37−39] and thus, steady-state asymmetry of plasma membrane lipids is assumed to be lost in viral particles.

Previously, we showed that the impediment to membrane fusion of Serinc5-containing HIV pseudoviruses is overcome by incorporation of the exogenous lipid Atto488-dimyristoyl PE (Atto488-DMPE) and treatment with the lipophilic antifungal drug amphotericin B, while fusion of HIV particles containing the non-restricting paralogue, Serinc2, is unaffected by these additions.[3] These data suggest that Serinc5 restriction may be dependent on the lipid environment of the viral membrane. To address the hypothesis that Serinc5 alters lipid bilayer properties of the HIV envelope, we systematically investigated the effects of Serinc5 incorporation on membrane order of pseudoviral particles and the physical and chemical properties of lipids required to overcome restriction by Serinc5.

RESULTS

Serinc5 Increases Lipid Acyl Chain Order in the Viral Membrane. To examine the effects of Serinc incorporation on the order and tension of the HIV lipid bilayer, we labeled HIV pseudovirus particles with the fluorescent membrane dye FLIPPER-TR. While FLIPPER-TR has been described as a reporter of membrane tension, it also reports on acyl chain packing in model or biological membranes. Viral membranes lack the typical sources of tension in cellular membranes (hydrostatic, cytoskeleton interactions, and adhesion), although it is possible that the HIV matrix protein (MA) introduces tension in the viral membrane.[11] Thus, in the context of viral membranes, FLIPPER-TR may primarily function as a reporter of membrane order and elastic modulus, that is, membrane biophysical properties that are all interrelated. This push-pull fluorescent probe changes wavelength (red-shifted excitation) and has a longer lifetime in membranes with increased lipid order.[32,40,41] FLIPPER-TR has been used as a reporter of membrane order not only in lipid model membranes but also in a variety of biomembranes.[32,40,42] To calibrate the FLIPPER-TR method for application to pseudoviruses, which appear as diffraction-limited spots by fluorescence microscopy, we first measured the fluorescence lifetimes of FLIPPER-TR-stained large unilamellar vesicles (LUVs) of comparable size to pseudoviruses (Figure 1, left and Figure S1) by fluorescence lifetime imaging microscopy (FLIM). LUVs were made of ternary lipid compositions previously reported to exist as all L_o, all L_d, or co-existing L_o/L_d phases.[43,44] As expected, we observed longer, shorter, and intermediate average lifetimes for L_o, L_d, and L_o/L_d LUVs, respectively (Figure 1, left). The measured lifetimes of FLIPPER-TR in all LUVs studied here are shorter than previously reported lifetimes in membrane vesicles with a larger diameter, which may be due to altered pressure profiles and elastic moduli in vesicles with decreasing diameters.[45,46] The lifetimes of FLIPPER-TR in these LUVs composed of varying ratios of SM, cholesterol, and palmitoyl-oleoylphosphatidylcholine (POPC) were also comparable to LUVs with simpler compositions known to exist as all L_o, all L_d, or co-existing L_o/L_d phases (Figure S2).

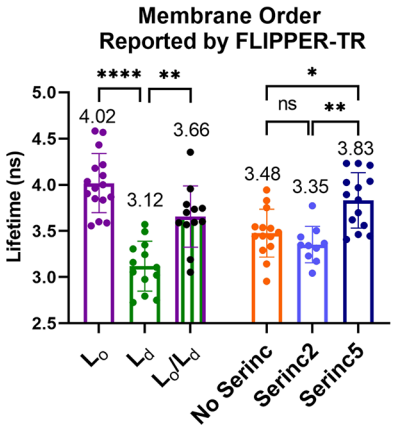

Figure 1. Fluorescence lifetimes of the lipid order sensitive membrane dye, FLIPPER-TR, in liposomes of defined lipid composition and in HIV pseudovirus particles. Large unilamellar liposomes (LUVs) composed of ternary mixtures of the major lipid components of the HIV envelope in ratios known to exist solely in L_o (35/40/25, SM/chol/POPC), solely L_d (25/5/70, SM/chol/POPC), or as a mixture of L_o and L_d (40/20/40, SM/chol/POPC) phases were used as standards for comparison. LUVs and HIV pseudoviruses were stained with FLIPPER-TR, adhered to a coverslip, and imaged by fluorescence microscopy. The fluorescent puncta were segmented from the background by intensity thresholding, and the average lifetimes of all particles within a field of view are plotted as a point with mean and SD of all data points of identically prepared samples. The mean lifetime in nanoseconds of all data points for a condition is written above each bar. Data are from at least three independent preparations of LUVs and pseudoviruses. Multiple comparisons by Dunnett's T3 multiple comparisons test: ****$p < 0.0001$, **$p < 0.01$, *$p < 0.05$, ns not significant.

HIV pseudoviruses were stained with FLIPPER-TR and imaged in the same manner by fluorescence lifetime microscopy. The lifetimes of the dye in pseudovirus membranes without Serincs or with Serinc2 (Figure 1, right, orange and light blue circles, respectively) were similar to those in LUVs with coexisting L_o and L_d phases, whereas the lifetimes in pseudovirus membranes that incorporate Serinc5 were longer, indicating more ordered membranes (Figure 1, right, dark blue circles). These data show that unrestricted HIV pseudoviral membranes exhibit lipid chain order intermediate between the L_o and L_d extremes of model membranes and further support the hypothesis that Serinc5, but not Serinc2, alters the organization of lipids within the viral membrane to become more ordered.

https://doi.org/10.1021/acsinfecdis.2c00478
ACS Infect. Dis. 2023, 9, 773−784

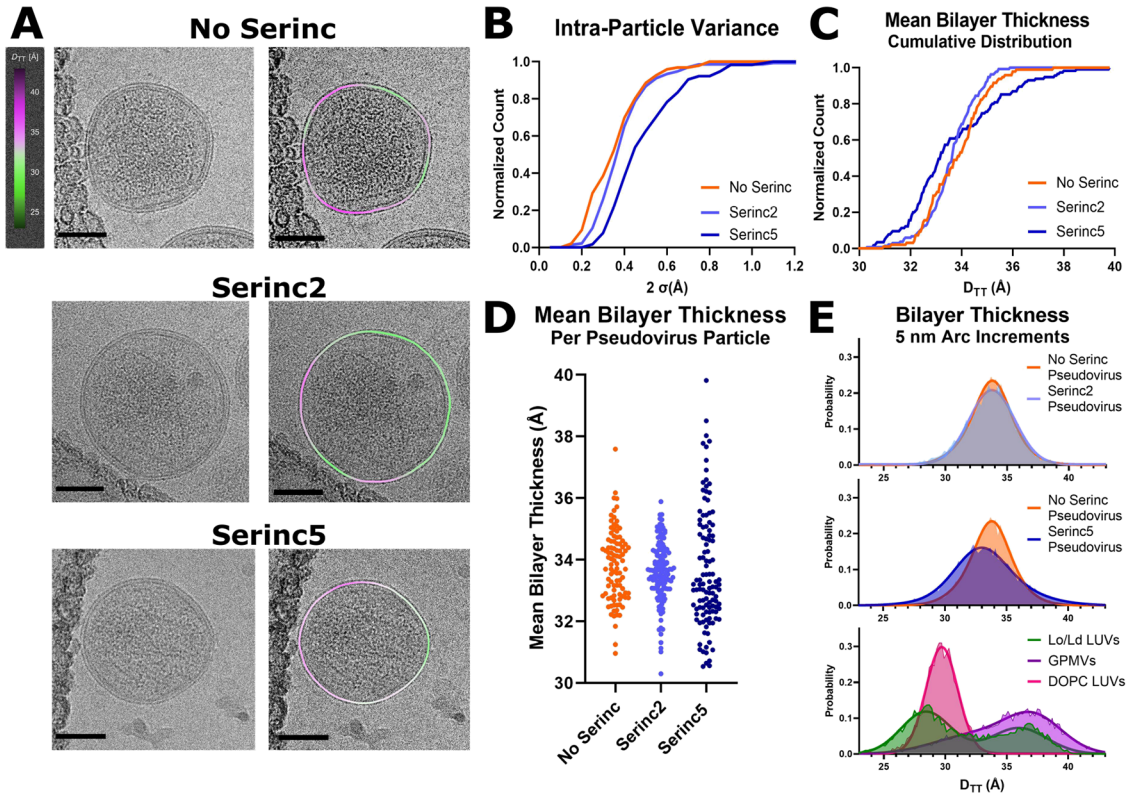

Figure 2. Serinc5 incorporation increases membrane heterogeneity and widens the thickness distribution of HIV pseudovirus particles as measured by cryoEM. (A) Example micrographs (left) with membrane thickness (D_{TT}) overlay (right) of HIV pseudoviruses prepared without Serincs (No Serinc), with Serinc2, or with Serinc5. The measured distances between intensity troughs (D_{TT}) for 5 nm segments of the membranes were plotted as a smoothed, colored overlay according to the scale on the left. Scale bars are 50 nm. (B) 95% confidence intervals of the mean bilayer thickness (D_{TT}) of individual HIV pseudovirus particles plotted as a cumulative distribution function. Mean membrane thickness (D_{TT}) of individual HIV pseudoviruses plotted as a cumulative distribution function (C) and as a bee swarm plot (D). Each point represents one pseudovirus particle. Data are combined from at least two independent preparations of pseudoviruses with over 100 viral particles analyzed for each condition. (E) Normalized distributions of membrane thickness (D_{TT}) measurements of 5 nm segments of HIV pseudovirus, LUV, or giant plasma membrane vesicle (GPMV) membranes with double Gaussian fits. One-phase LUVs were composed of DOPC/POPG (95/5 molar ratio), and two-phase LUVs were composed of a 40/20/35/5 ratio of DPPC/chol/DOPC/POPG. LUV and GPMV distributions adapted with permission from ref 34 copyright year 2020.

Viral Membrane Thickness Is Heterogeneous and Serinc5 Broadens the Viral Membrane Thickness Distribution. To examine the effects of Serinc5 incorporation on viral membranes at higher resolution, we turned to recently developed techniques for visualizing membrane heterogeneity by cryoEM.[34] Increased membrane order is usually accompanied by an increase in membrane thickness. However, it is not trivial to measure thickness in biological membrane samples, especially if the membrane itself contains coexisting areas of variable thickness. This problem can be overcome by applying cryoEM to LUVs and biologically derived membranes.[34,35] To detect membrane thickness variation in the envelopes of HIV pseudovirus particles, we flash-froze particles that incorporated Serinc2, Serinc5, or no Serincs and imaged them by cryoEM (Figure 2). The membrane envelopes of the particles are characterized by two lines of high density, or "troughs" (Figure S4C). The trough-to-trough distance (D_{TT}) was previously found to match most closely with the hydrophobic thickness of the bilayer when compared with small-angle X-ray scattering,[34] suggesting that the trough position corresponds roughly to the glycerol backbone region of the bilayer. D_{TT} of the viral membrane in these projection images was measured in 5 nm segments as described previously[34] and example micrographs with D_{TT} heat maps are shown in Figures 2A and S3. We also frequently observe a line of density under the thinner portions of the membrane at a distance that is consistent with the MA of HIV (Figure S4).

The majority of particles from all three preparations show intra-particle variations in membrane thickness with contiguous areas of thicker or thinner membrane within any particle cross-section. Cumulative distribution plots of the standard deviation of membrane thickness within individual particles reveals substantially greater intra-particle thickness variance for Serinc5 particles compared to particles with Serinc2 or without Serincs (Figure 2B). Averaging D_{TT} per particle, the mean bilayer thicknesses were similar for HIV particles with Serinc2 and without Serincs, but the distribution of thicknesses for Serinc5-containing pseudoviruses is much broader, with about 35% of all particles exhibiting thicker and about 65% thinner membranes than the average No Serinc or Serinc2 particle (Figure 2C,D), reinforcing and expanding on the fluorescence lifetime data shown in Figure 1. The broader distribution of membrane thicknesses in Serinc5 particles may be attributable to the known variability in Serinc5 incorporation into individual particles.[4] The distribution of particle sizes is comparable for HIV pseudoviruses with and without Serincs, and we detected no relationship between particle size and mean membrane thickness (Figure S5). When the

https://doi.org/10.1021/acsinfecdis.2c00478
ACS Infect. Dis. 2023, 9, 773−784

thicknesses of 5 nm segments of all analyzed pseudoviral membranes are plotted as probability histograms, the distributions of viral particles without Serincs and with Serinc2 are practically identical, while the distribution from Serinc5-containing particles is broader, that is, containing more regions of both thinner and thicker membrane areas (Figure 2E). Comparing these pseudoviral distributions to previously published distributions of LUV and GPMV membranes,[34] all pseudoviral distributions show a single peak that is more broadly distributed than single phase LUVs, but still not as broadly distributed as GPMVs (Figure 2E). While the pseudoviral distributions are centered between the L_d and L_o peaks of the two-phase LUVs, the GPMV distribution is skewed toward L_o-like thicknesses. While membrane thicknesses in neither pseudoviral particles nor GPMVs were clearly bimodally distributed as they are in the two-phase LUVs, the broad distributions suggest a higher complexity in the lipid phase behavior of biological compared to model membranes. Broader distributions would also result if domain sizes were smaller and more numerous because out-of-plane domains of different thicknesses may appear as intermediate thickness in projection images. As domain size approaches the segment length of the analysis (5 nm), the probability increases that a segment contains densities of both phases, resulting in more segments with intermediate thickness and thus a broader unimodal distribution rather than a clearly bimodal distribution.

Treatment of the HIV Pseudoviral Membrane with PE Reverses Serinc5's Fusion Inhibition by Decreasing Membrane Heterogeneity and Order. We used a previously described total internal reflection fluorescence (TIRF) microscopy-based, single-particle fusion assay to examine the effects of treatment of HIV pseudovirus particles with an aqueous suspension of phospholipids (Figure 3A). Briefly, binding of pseudovirus particles engineered to incorporate an mCherry content marker to a supported planar plasma membrane containing CD4 receptor and CCR5 co-receptor produces a sudden appearance of punctate fluorescence in the observed evanescent field. After remaining stably bound for several imaging frames, the particle either fuses, as reported by a decay of fluorescence as the mCherry content diffuses away over multiple frames of recorded video, or becomes unbound from the membrane, reported by a sudden drop in fluorescence intensity back to baseline over a single frame. We have previously established strong concordance between fusion of HIV pseudoviruses in this assay with in vitro infection efficiency, including particles with or without Serincs.[3] Additionally, we showed that treatment with the polyene antifungal, Amphotericin B, which has complex interactions with membranes, increases infection and fusion of Serinc5-containing HIV pseudoviruses.[3] Similarly, labeling HIV pseudoviruses with the fluorescent lipid, Atto488-dimyristoylphosphatidylethanolamine (DMPE), increased fusion capability of Serinc5-containing HIV pseudoviruses (Figure 3B reproduced from ref 3). DMPE modified at the headgroup with Atto488 is chemically distinct from unmodified DMPE, so we assessed the effects of exogenous unmodified DMPE on fusion of HIV pseudoviruses incorporating Serinc5, Serinc2, or no Serinc (Figure 4A) and found the same reversal of Serinc5's inhibition of HIV membrane fusion. Additionally, we compared the effects of acyl chain length and saturation by examining the fusion of pseudoviruses treated with dipalmitoyl, dioleoyl, and palmitoyl-oleoyl PE. Both saturated [DMPE and 1,2-dipalmitoyl-sn-glycero-3-phosphoethanolamine (DPPE)] and unsaturated (1,2-dioleoyl-sn-glycero-3-phosphoethanolamine, DOPE) lipids increased fusion of Serinc5-containing pseudoviruses with only minimal effect on pseudoviruses without Serincs or with Serinc2. Thus, restoration of fusion of Serinc5-containing pseudoviruses upon treatment with PE is a function of the PE headgroup independent of acyl chain length or saturation.

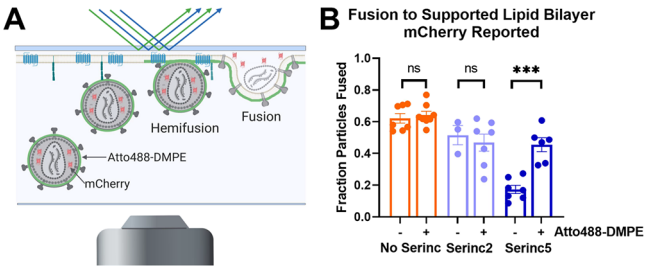

Figure 3. Lipid composition of the viral membrane affects Serinc restriction of HIV membrane fusion. (A) Diagram of TIRF microscopy-based single HIV pseudovirus particle fusion assay. Pseudovirus binding to a supported planar plasma membrane containing CD4 receptor and CCR5 co-receptor is reported as a sudden appearance of bright puncta that remain stationary for several imaging frames. Fusion is reported by a decrease in fluorescence over several imaging frames as a genetically encoded content marker, mCherry, diffuses away. (B) Incorporation of Atto488-DMPE increases fusion of HIV pseudovirus particles containing Serinc5 but does not affect fusion of particles without Serinc or containing Serinc2. Each data point represents the fraction of particles fused on a separately prepared bilayer. Reproduced from ref 3, copyright year 2020. ***, $p < 0.001$; ns, not significant by multiple unpaired t-tests via the Holm−Sidak method. Each condition includes data from at least three distinct preparations of pseudovirus.

To further confirm that the PE headgroup is critical to counteract the fusion restriction of Serinc5, we treated particles with palmitoyl-oleoylphosphatidylcholine (POPC) or palmitoyl-oleoyl-phosphatidylserine (POPS) and found that these lipids had no effect on fusion of any pseudoviruses tested (Figure 4A). While fewer particles incorporated fluorescently labeled PC than PE or PS (Figure S6A,C) and the amount of PC incorporated was lower than the amount of PE or PS (Figure S6B), PS incorporation was equal to PE incorporation yet still failed to increase fusion of Serinc5-containing particles, indicating the specificity of PE in overcoming Serinc5-restriction of HIV membrane fusion. Due to their smaller headgroup, negative membrane curvature-inducing and hydrogen bonding capability, PEs are known to alter the lateral pressure profile and hence membrane bending elasticity of lipid bilayers.[47]

To better understand the mechanisms underlying the reversal of Serinc5's inhibition of HIV fusion by PE enrichment, we applied the FLIM and cryoEM assays described above to assess membrane order of Serinc5-containing pseudoviruses that had been treated with PEs of varying chain length and saturation (Figures 4B,C and S7). DMPE is a lipid with two saturated 14-carbon chains and DOPE is an unsaturated lipid with two 18-carbon chains with one *cis* double bond each. Compared to untreated Serinc5-containing pseudovirus particles, DMPE and DOPE-treated particles had a clear trend to shorter FLIPPER-TR lifetimes with DMPE treatment showing a significant difference from untreated (Figure 4B). Imaging the same PE-treated viral

https://doi.org/10.1021/acsinfecdis.2c00478
ACS Infect. Dis. 2023, 9, 773−784

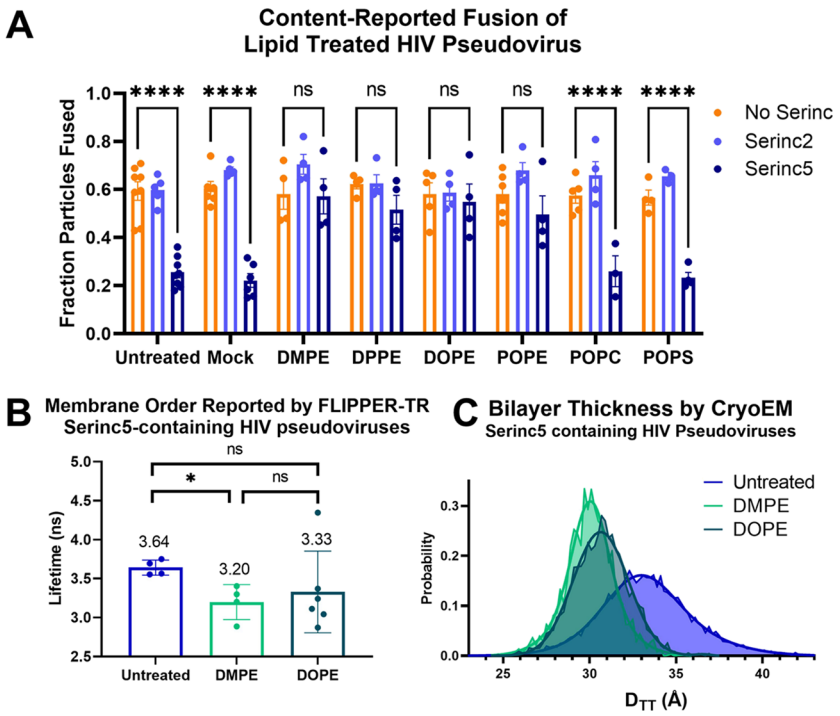

Figure 4. Treatment of HIV pseudoviruses with PE overcomes restriction of fusion of Serinc5-containing particles by decreasing membrane heterogeneity and order. HIV pseudoviruses with or without Serincs were treated with aqueous suspensions of the lipids listed on the *X*-axis, separated from free lipids, and (A) fusion with supported plasma membranes was assessed by TIRF microscopy-based single-particle membrane fusion. A two-way ANOVA test was conducted to examine the statistical significance of the effects of Serinc incorporation and lipid enrichment on HIV pseudovirus fusion. There was a statistically significant interaction between the two factors, $F(14, 88) = 4.894$, $p < 0.001$. Tukey's multiple comparisons test showed very significant differences in the means of the comparisons shown above (****$p < 0.0001$, ns not significant). None of the No Serinc-Serinc2 comparisons were significant. Each data point represents the fraction of particles fused on a separately prepared supported membrane. Each condition includes data from at least three distinct preparations of pseudovirus. (B) Fluorescence lifetimes of FLIPPER-TR in lipid-treated, Serinc5-containing HIV pseudoviruses. HIV pseudoviruses containing Serinc5 were stained with FLIPPER-TR after treatment with the lipid listed on the *X*-axis and imaged by fluorescence microscopy as in Figure 1. Each data point is the result obtained from one field of view within a sample and is plotted with mean and standard deviation. Statistical significance by Welch's unpaired t-test: *$p < 0.05$, ns not significant. (C) Normalized distributions of membrane thickness (D_{TT}) measurements of 5 nm segments of the same preparation of Serinc5-containing HIV pseudoviruses treated with the lipid listed in the key as panel (B) and their corresponding double-Gaussian fits. The untreated Serinc5 distribution is replotted from Figure 2E for comparison.

particles by cryoEM revealed that there was a marked decrease in membrane thickness (as measured by D_{TT}) for both PEs (Figure 4C), echoing the decrease in membrane order reported by FLIPPER-TR. Additionally, the PE-treated Serinc5 particles had much lower variance in membrane thickness than untreated particles (Figure S7C). From these data, it appears that treatment with exogenous PE reverses Serinc5's increase in membrane order and heterogeneity to restore the particles' membrane fusion capability.

DISCUSSION

In this study, we sought to better understand the mechanism by which Serincs restrict HIV membrane fusion and entry of HIV particles into cells. We previously established that Serinc5, but not Serinc2, inhibits fusion pore opening and constricts the widening of the fusion "neck" of virus particles fusing with plasma membranes that were derived from HIV receptor and co-receptor expressing cells.[3] Changes in the function of Env would be expected to primarily affect the early steps of membrane fusion that are dependent on conformational rearrangements of Env. However, the final step, pore enlargement, is thought to occur after all conformational rearrangements of Env are complete and thus is dependent on membrane properties such as curvature and line tension for energy input.[11] Serinc-dependent changes to the properties of the viral membrane could explain the observed defects in fusion pore dilation with viral envelopes containing Serinc5.

To reveal more insightful details on the mechanism by which Serincs inhibit virus entry, we employed fluorescence lifetime imaging and cryoEM methods to assess the importance of lipid order in the viral membrane for Serinc5's inhibition of HIV membrane fusion. While HIV pseudoviral membranes with and without the non-restricting isoform, Serinc2, were nearly identical by FLIPPER-TR-reported membrane order (Figure 1) and cryoEM-measured membrane thickness (Figure 2B–E, top panel), pseudoviral membranes that incorporated Serinc5 were more ordered (Figure 1) and more heterogeneous (Figure 2B), and had a broader interparticle thickness distribution by cryoEM (Figure 2C,D), with many more regions of increased and decreased membrane thickness than viral envelopes with Serinc2 or no Serincs (Figure 2E, middle panel). These two techniques report on slightly different properties of membranes, and while the direction of the changes they report are consistent, their magnitudes differ, as is common for techniques measuring membrane order.[48] More specifically, three factors could reconcile the broader thickness distributions observed by cryoEM and the increased lipid order measured by

https://doi.org/10.1021/acsinfecdis.2c00478
ACS Infect. Dis. 2023, 9, 773−784

fluorescence lifetime imaging. First, as mentioned above, overlapping areas of L_o and L_d phases that are too small to be resolved in cryoEM projection images will lead to an apparent broadening of the membrane thickness distributions measured by cryoEM. Second, domain sizes may fluctuate in space and time and these fluctuations may be beyond the resolution of cryoEM such that observed thicknesses are blurred over those of fluctuating segments. Third, a more favorable partitioning of FLIPPER-TR into L_o than into L_d domains or perhaps a more complex behavior of the probe at lipid domain interfaces may explain the increased order measured in the Serinc5 particles. Notably, Raghunath et al.[49] failed to detect increased membrane heterogeneity in Serinc5 containing HIV particles with fluorescent membrane order probes that report solvent accessibility, a membrane property that is frequently but not always related to membrane order.[50] Despite these caveats, we demonstrate with two techniques that increased heterogeneity in the viral membrane only occurred with incorporation of the restricting isoform, Serinc5, and not the non-restricting isoform, Serinc2, which strongly suggests that the restriction function of Serinc5 is related to altered lipid order and organization in the viral membrane.

Our observation that PE treatment increases fusion of Serinc5-containing viruses (Figure 4A) is further demonstration of the importance of altered membrane properties for Serinc5-mediated fusion inhibition. The reversal of Serinc5's function with PE treatment is accompanied by a reversal of Serinc5's effects on viral membrane organization with decreased order reported by FLIPPER-TR (Figure 4B) and dramatically reduced membrane thickness by cryoEM (Figure 4C). Again, these two techniques report on slightly different properties of ordered/disordered membranes, so while the magnitude of the effect of PE enrichment is different between the two measures, the overall direction of the change is consistent—PE treatment reduces membrane order regardless of acyl chain length or saturation. This effect may be due to trace exogenous phospholipid incorporation into the viral membrane as suggested by fluorescent analogues (Figure S6) likely with preferential enrichment in the external leaflet of the viral membrane (ref 3, Figure S6), which could alter several membrane properties including intrinsic curvature, lateral tension, and line tension that influence lipid nanodomains and fusion.[47,51,52] Alternately, treatment with the lipid particle suspension may extract some lipid species from the viral membrane, such as cholesterol, which could also affect membrane order and fusion. Regardless, the data suggest that altered membrane order and heterogeneity is essential for Serinc5's restriction of HIV membrane fusion.

The observation of coexistence of thicker and thinner membrane domains in HIV pseudoviral membranes (Figures 2 and S3) is, to our knowledge, the first time that domain coexistence has been directly observed in a viral membrane. Previous bulk measurements of lipid order of HIV particles have shown the membrane to be largely ordered, but that lipid order in HIV particles also depends on the producing cell line.[53] Phase separation has been observed in supported lipid bilayers made from viral membrane lipid extracts,[26] but not in intact viral particles. Building on our observation of membrane heterogeneity in the HIV envelope, we note a line of density (Figure S4) at a distance from the bilayer consistent with an incomplete MA layer of HIV.[54,55] Prior reconstitution experiments have shown thinning of the bilayer upon MA binding to model membranes[56] and similarly, we observe MA density most frequently under thinner portions of the viral membrane, thus recapitulating prior reconstitution data in intact viral particles. It is possible that the underlying MA layer introduces tension and further changes the mechanical properties of the viral envelope, however, a more detailed analysis of MA dependent effects on the viral envelope is beyond the scope of the current study.

It has been shown previously that both Env and Serinc5 partition into membrane domains with more ordered lipids[5,57] and that Serinc5 disrupts the clustering of Env in the viral membrane.[8] If clustering in the mature viral envelope is driven by confinement of Env to small, ordered lipid domains, increasing area or fragmentation of ordered domains could reduce clustering, thus decreasing the number of Env trimers available to catalyze fusion.[58] Additionally, Serincs have been hypothesized to alter Env conformation as demonstrated by multiple methods.[4−8,59,60] Changes in Env conformation, especially increased exposure of the membrane proximal external region of Env, could also be a result of altered membrane thickness and order.[61]

As a result of increased order, the Serinc5 viral membrane is likely stiffer than a viral membrane without Serincs,[62] potentially explaining arrest of membrane fusion at highly curved intermediates (Figure 5). Additionally, changing area

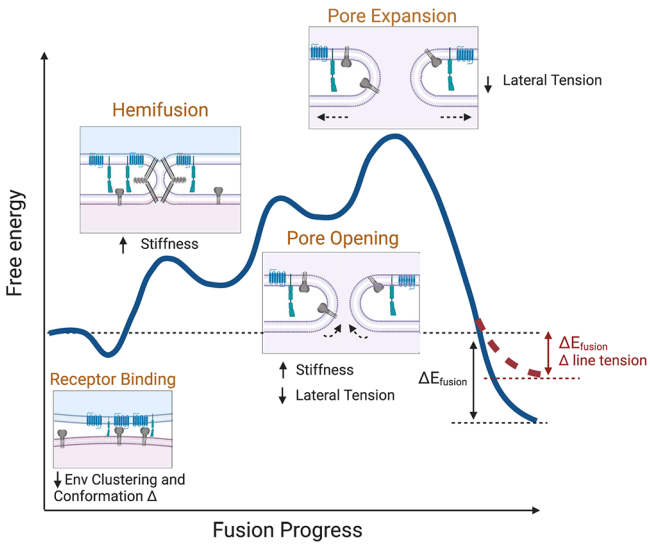

Figure 5. Model of energy changes to fusion resulting from Serinc5-induced increase in membrane heterogeneity of the viral envelope. The approximate free energy change of intermediate steps (orange titles) along the fusion reaction is shown by the blue line. Proposed effects of Serinc5-induced alterations of membrane physical properties are listed in black near each intermediate state. Many of these properties are inter-related and are not easily disentangled. The effect of increased membrane heterogeneity on the contribution of line tension to the energetics of fusion is shown by the red dashed line.

fraction and distribution of ordered lipid domains may reflect altered line tension between domains in the viral membrane.[63] Previous work from our laboratory has shown that in phase-separated viral and target membranes, the energy of line tension can drive HIV gp41-mediated fusion, that this effect depends on the size and distribution of ordered domains in the target membrane, and that increasing ordered domain area in a viral particle beyond its optimum would be expected to inhibit fusion.[52] Applying this simplified model to study the effect of

https://doi.org/10.1021/acsinfecdis.2c00478
ACS Infect. Dis. 2023, 9, 773−784

increased ordered domain area in the membrane of a viral particle with 110 nm diameter, we found that increasing the fraction of the membrane in an ordered domain first increases and then sharply decreases the contribution of line tension to the free energy change of fusion (Figure S8). It is well known that the final step of fusion, fusion pore expansion, is dependent on lateral tension in the membrane.[11,64−67] In a more ordered membrane, the elastic modulus would be expected to change along with altered curvature and line tension, all of which affect the energy profile for membrane fusion.[47,68] Decreased lateral tension would also be expected to inhibit fusion pore expansion, resulting in the increased frequency of early fusion products observed with cinched membranes.[3]

Serinc 3 and 5's possible functions as lipid binding and/or translocating integral membrane proteins[25,59,69] could alter effective lipid concentrations and asymmetry in the viral membrane, and thus alter lipid order. Specifically, Serincs 3 and 5 may alter the distribution of PE across the two leaflets of the viral membrane. PE is known to enhance membrane fusion, especially when preferentially incorporated into the two contacting leaflets of fusing membranes.[51,70,71] As a cone-shaped molecule, PE induces frustrated negative curvature in the pre-fusion membrane, increasing lateral tension in the headgroup region.[47] In support of this hypothesis, we showed that addition of PE can overcome Serinc5's inhibitory function on fusion (Figure 4A) and that this was accompanied by larger changes in membrane order that likely promote fusion as well. The fundamental and unifying change underlying the potential hypotheses for Serinc 3 and 5's mechanism of action is increased viral membrane heterogeneity.

Previously, we hypothesized that Serinc5 would need to cause "broad energetic changes" to the membrane fusion process to accumulate arrested intermediates at every step, as we observed.[3] With the data presented here, we show that Serinc5 increases viral membrane heterogeneity and that this is necessary for the partial inhibition of HIV fusion. Contextualizing previous observations and hypotheses about Serinc5's mechanism of action with our data, we posit that alteration of membrane order underlies the other effects of Serinc5 incorporation into the HIV envelope. Following from this, whether agents that increase membrane order could be effective anti-HIV therapeutics needs further study.

METHODS

Cell Lines, Reagents, and Plasmids. HEK 293 T/17 cells (ATCC) were maintained in high glucose Dulbecco's Minimum Essential Media (Gibco) supplemented with 10% fetal bovine serum (Atlanta Biologicals), 1% antibiotic-antimycotic (Gibco), 1 mM sodium pyruvate (Gibco), and 2 mM glutamine (Gibco). CD4 and CCR5 overexpressing HeLa cells (gift of David M. Rekosh, University of Virginia) were maintained in Iscove's Modified Dulbecco's Medium (Gibco) supplemented with 10% fetal bovine serum and 1% antibiotic/antimycotic with 0.5 mg/mL of G418 (Gibco), and 1 μg/mL puromycin. All cells were maintained at 37 °C with 5% CO_2 atmosphere.

pHIV-luciferase, pHIV-Rev, and pHIV-pack were gifts of Wen Yuan (University of Virginia). pHIV-Env-SF162 was provided by the AIDS Reagent Program. pHIV-imCherry[72] was a gift of Gregory Melikian (Emory University). pPBJ5-Serinc2-HA was a gift of Massimo Pizzato (University of Trento), and pPBJ5-Serinc5-HA was a gift of Heinrich Gottlinger (University of Massachusetts Medical School, Worcester).

The following compounds were purchased from Avanti Polar Lipids and used without modification: brain PC (bPC), egg SM, 1-palmitoyl-2-oleoyl-sn-glycero-3-phosphoethanolamine, DOPE, 1,2-dimyristoyl-sn-glycero-3-phosphoethanolamine (DMPE), DPPE, 1-palmitoyl-2-oleoyl-glycero-3-phosphocholine (POPC), 1,2-dipalmitoyl-sn-glycero-3-phosphocholine (DPPC), 1-palmitoyl-2-oleoyl-sn-glycero-3-phospho-L-serine (POPS), 1-palmitoyl-2-oleoyl-sn-glycero-3-phospho-(1′-rac-glycerol) (POPG), 1-palmitoyl-2-{6-[(7-nitro-2-1,3-benzoxadiazol-4-yl)amino]hexanoyl}-sn-glycero-3-phosphocholine, 1-palmitoyl-2-{6-[(7-nitro-2-1,3-benzoxadiazol-4-yl)-amino]hexanoyl}-sn-glycero-3-phosphoserine, and 1-palmitoyl-2-{6-[(7-nitro-2-1,3-benzoxadiazol-4-yl)amino]hexanoyl}-sn-glycero-3-phosphoethanolamine. Cholesterol was purchased from Sigma-Aldrich. 1,2-dimyristoyl-*sn*-glycero-3-phosphoethanolamine-PEG3400-triethoxysilane was synthesized as described previously.[73]

HIV Pseudovirus Preparation. HIV pseudoviruses were produced as described before by transfection of HEK 293 T cells (ATCC) with Lipofectamine 2000 (Invitrogen) and the following amounts of plasmids per 10 cm dish: 13 μg of pHIV-luciferase, 5 μg of pHIV-pack, 4 μg of pHIV-Env-SF162,[74−76] 4 μg of pHIV-imCherry, 1 μg of pHIV-Rev, and 4 μg of pBJ5-Serinc2-HA[1] or pBJ5-Serinc5-HA,[2] as indicated in text. pHIV-pack expresses the major HIV-1 polyproteins, Gag and Pol, while Env and Rev. are expressed from separate plasmids. Additionally, a fluorescently tagged version of HIV gag is included to enable reporting of post-fusion content release in the TIRF-based fusion assay and luciferase under the HIV-1 5′ long terminal repeat to allow easy titering of pseudovirus preparations. Culture media was changed 4−6 h after transfection to phenol-red free DMEM supplemented with 10% FBS, 1% antibiotic-antimycotic, 1 mM sodium pyruvate, and 2 mM glutamine. Culture supernatants were harvested 2 days after transfection and cleared by centrifuging 5000 × *g* before passing through a 0.22 μm filter. HIV pseudoviruses were pelleted through a 25% sucrose-HME [20 mM HEPES, 20 mM morpholinoethanesulfonic acid, 130 mM NaCl, 1 mM EDTA (pH 7.4)] cushion, as previously described,[77] and resuspended in buffer HME without sucrose. Pseudovirus preparations for cryoEM were further purified by density dependent centrifugation on a discontinuous sucrose gradient composed of 65% sucrose-HME and 25% sucrose-HME spun 151,000xg for 18 h. Pseudovirus was collected from the 65%/25% sucrose interface, diluted in buffer HME without sucrose, and repelleted through a 25% sucrose cushion. After resuspension in buffer HME without sucrose, the pseudovirus preparation was aliquoted and stored at −80 °C. Additionally, the concentration of HIV p24 in each preparation was measured by ELISA[78,79] and used to normalize the amount of pseudovirus added to downstream experiments. Quantification of Serinc incorporation into pseudoviral particles prepared in the same manner is shown in Figures S3 and S8 of ref 3. While Serinc5 incorporates into viral particles more readily than other Serincs, there is no relationship between the level of Serinc incorporation and restriction activity[80] for Serinc levels above a low threshold.[3]

Lipid Treatment of HIV Pseudoviruses. 10^{-10} moles of the indicated lipid were dried on the bottom of a glass test tube to remove chloroform/methanol solvent and resuspended by vigorous vortexing in buffer HB [20 mM HEPES, 150 mM

https://doi.org/10.1021/acsinfecdis.2c00478
ACS Infect. Dis. 2023, 9, 773−784

NaCl (pH 7.4)] to yield a concentration of 1.4 μM. 21 ng of HIV pseudovirus, as measured by p24 ELISA, was mixed with the lipid suspension. The mixture was incubated at room temperature for 2 h on a rotary spinner. To remove free lipid, the HIV pseudovirus mixture was diluted up to 1.5 mL in buffer HB and pelleted by spinning at 21,000 × g for 1 h at 4 °C before final resuspension in buffer HB. Lipid-treated HIV pseudoviruses were used within 24 h.

LUV Preparation. Chloroform stocks of desired lipids were mixed, and the solvent was evaporated under a gentle stream of nitrogen gas. The resulting lipid film was desiccated under vacuum for at least 1 h before resuspension in buffer appropriate to the experiment to a final concentration of 1 mM. After vortexing at room temperature, the lipid suspension was subjected to 10 freeze/thaw cycles in liquid nitrogen and warm water before extrusion through two 100 nm polycarbonate membranes (Avestin). Resulting LUVs were stored at 4 °C and used within 24 h of extrusion.

Plasma Membrane Bleb Preparation. Blebs were produced from HeLa cells overexpressing CD4 and CCR5 by previously published methods.[20,81] Briefly, when cells reached 90% confluence, they were washed twice with blebbing buffer (10 mM HEPES, 150 mM NaCl, 2 mM $CaCl_2$, pH 7.4) and blebbing was induced by replacing buffer on the cells with 5 mL of 25 mM formaldehyde (J.T.Baker) and 2 mM dithiothreitol (DTT) diluted in blebbing buffer and incubating the cells at 37 °C, 5% CO_2 for 1 h. After an hour, blebs were detached from cells by shaking on a radial shaker at room temperature for 1 h before the supernatant was collected and cleared of large cell debris by centrifuging at 100 × g for 10 min. Blebs were pelleted at 20,000 × g for 1 h and washed twice in blebbing buffer without DTT or formaldehyde.

TIRF Supported Lipid Bilayer Fusion Assay. Supported planar plasma membranes derived from blebs were prepared as previously described.[20,73,82] Quartz slides were cleaned in piranha solution (95% H_2SO_4 and 30% H_2O_2 in a 3:1 ratio) and rinsed in 12 liters of deionized water. Next, a lipid monolayer composed of 4:1 bPC and cholesterol (Avanti Polar Lipids) with 3% 1,2-dimyristoyl-*sn*-glycero-3-phosphoethanolamine-PEG3400-triethoxysilane was deposited on the quartz slide by the Langmuir−Blodgett method. A chloroform solution of the lipid mixture was applied to a Nima 611 Langmuir−Blodgett trough, and after letting the solvent evaporate for 10 min, the lipid layer was compressed at a rate of 10 cm^2/min to a pressure of 32 mN/m. A cleaned, rinsed, and dried quartz slide was rapidly dipped (68 mm/min) and slowly removed (5 mm/min) from the trough and then dried in a desiccator chamber overnight.

The slide was then assembled into a custom-built microscopy flow cell and plasma membrane blebs diluted in blebbing buffer without DTT or formaldehyde were flowed in to form the outer leaflet of the supported planar plasma membrane. After 1−2 h at room temperature, the flow cell was washed with multiple volumes of blebbing buffer, then multiple volumes of buffer HB, and transferred to a prism-based TIRF microscope (Zeiss AxioObserver Z1). The sample was excited with a 561 nm diode laser (OBIS 561 nm LS, Coherent) at an angle of 72 degrees from normal and emission light was filtered through a dichroic mirror (DC565, Semrock) and a band-pass filter (BP605/50, Semrock). The video was recorded by an EMCCD (DV887ESC-BV, Andor Technology) in frame transfer mode with an exposure time of 0.2 s for 13.3 min as a dilution of HIV pseudovirus totaling 21 ng of p24 as measured by ELISA was flowed into the chamber. Laser intensity, shutter, and camera were controlled by a custom LabView program (National Instruments).

Intensities of single particles over time were extracted with a custom-built LabView program and classified as representing binding without fusion or binding with fusion based on the criteria described in ref 3.

FLIM Data Acquisition and Analysis. HIV pseudoviruses and LUVs were stained with 500 nM FLIPPER-TR (Cytoskeleton Inc.) for 2 h at room temperature. Pseudoviruses and LUVs were resuspended in buffer HB and added to a poly-L-lysine-coated coverslip. After liposomes and pseudoviruses were allowed to settle and adhere to the coverslip for 30 min, an unbound sample was washed in buffer HB. Samples were imaged on a Leica Stellaris8 microscope with an 80 MHz pulsed white light laser, HyD detector, and FALCON software. The background was subtracted by intensity thresholding, and the fluorescence lifetime of all pixels above the intensity threshold within the field of view was fit with two components per the n-component reconvolution with IRF function within Leica LAS-X software. Only the longer component is displayed, as this is the more sensitive reporter of membrane order and tension.[32] For data collected in bulk (Figure S2), LUVs were stained in the same manner but added to a quartz cuvette instead of a coverslip and spectra were acquired in a Fluorolog-QM 75-22-C (Horiba, Canada) spectrofluorometer with a SuperK Extreme high power super continuum white laser (NKT Photonics) in time-correlated single photon counting mode. Laser repetition rate was 5.5 MHz. Spectra were again fit to a two-component exponential curve with background subtraction of a buffer only spectrum with the integrated PowerFit-10 decay analysis package (Horiba).

CryoEM of HIV Pseudovirus Particles. C-Flat 2/2-3C or 1.2/1.3-3C grids (Electron Microscopy Sciences) were glow-discharged at 10 mA for 90 s. A suspension of HIV pseudovirus in buffer HME was applied and blotted from the grid before freezing in liquid nitrogen cooled ethane. For initial experiments, LUVs composed of 20/40/35/5 Chol/DPPC/DOPC/POPG were spiked into the pseudovirus suspension before freezing to serve as internal standards for quality control. The grids were imaged on a Titan Krios electron microscope operating at 300 kV equipped with a K3/GIF (Gatan) and controlled by EPU software (ThermoFisher Scientific). Magnification was 33,000X, which yielded a pixel size of 2.7 Å. As described in ref 34, the optimal total dose was set at 13.8 e/Å^2. Micrographs were motion-corrected with MotionCorr2[83] (10 by 10 patch for 10 iterations with a tolerance of 0.5, dose weighted) before analysis of trough-to-trough distance as described previously.[34]

Calculation of the Contribution of Line Tension to Free Energy Change of Membrane Fusion. The previously described model to calculate the free energy change due to changes in line tension during fusion between phase separated membranes[52] was adapted to the parameters relevant to the presented experimental data. Specifically, fusion between a flat membrane and a vesicle of 110 nm diameter with one L_o and one L_d domain each, representing the plasma membrane and HIV viral membrane respectively. Assuming simple geometries without domain fluctuations, the boundary energy of an isolated domain is given by $E = \gamma L$, where γ is the line tension and L is the circumference of the domain.[84] Line tension in both membranes is assumed to be 1 pN[84] and the negative energy gain from line tension reduction (dE) relative

https://doi.org/10.1021/acsinfecdis.2c00478
ACS Infect. Dis. 2023, 9, 773−784

to k_BT ($-dE/k_BT$) was calculated for varying lipid domain sizes and fractions in both membranes. Depending on vesicle size, area fraction of L_o phase membrane, and domain sizes in the target membrane, fusion of the two membranes can result in an energy gain or energy cost from changes in line tension (Figure S8).

Statistical Analysis. All tests of statistical significance calculated in GraphPad Prism 9. Specific tests are listed in the figure legends.

■ ASSOCIATED CONTENT

Supporting Information

The Supporting Information is available free of charge at https://pubs.acs.org/doi/10.1021/acsinfecdis.2c00478.

Example fluorescence and cryoEM micrographs and model calculations (PDF)

■ AUTHOR INFORMATION

Corresponding Authors

Amanda E. Ward − *Department of Molecular Physiology and Biological Physics, University of Virginia Health System, Charlottesville, Virginia 22908, United States; Center for Membrane and Cell Physiology, University of Virginia, Charlottesville, Virginia 22908, United States;* orcid.org/0000-0001-8184-0447; Email: aew2fx@virginia.edu

Lukas K. Tamm − *Department of Molecular Physiology and Biological Physics, University of Virginia Health System, Charlottesville, Virginia 22908, United States; Center for Membrane and Cell Physiology, University of Virginia, Charlottesville, Virginia 22908, United States;* orcid.org/0000-0002-1674-4464; Email: lkt2e@virginia.edu

Authors

Daria Sokovikova − *Department of Molecular Physiology and Biological Physics, University of Virginia Health System, Charlottesville, Virginia 22908, United States; Center for Membrane and Cell Physiology, University of Virginia, Charlottesville, Virginia 22908, United States*

Melvin Neal Waxham − *Department of Neurobiology and Anatomy, The University of Texas Health Science Center at Houston McGovern Medical School, Houston, Texas 77030, United States;* orcid.org/0000-0003-4801-1190

Frederick A. Heberle − *Department of Chemistry, University of Tennessee, Knoxville, Tennessee 37996, United States;* orcid.org/0000-0002-0424-3240

Ilya Levental − *Department of Molecular Physiology and Biological Physics, University of Virginia Health System, Charlottesville, Virginia 22908, United States; Center for Membrane and Cell Physiology, University of Virginia, Charlottesville, Virginia 22908, United States;* orcid.org/0000-0002-1206-9545

Kandice R. Levental − *Department of Molecular Physiology and Biological Physics, University of Virginia Health System, Charlottesville, Virginia 22908, United States; Center for Membrane and Cell Physiology, University of Virginia, Charlottesville, Virginia 22908, United States*

Volker Kiessling − *Department of Molecular Physiology and Biological Physics, University of Virginia Health System, Charlottesville, Virginia 22908, United States; Center for Membrane and Cell Physiology, University of Virginia, Charlottesville, Virginia 22908, United States*

Judith M. White − *Department of Cell Biology, University of Virginia Health System, Charlottesville, Virginia 22908, United States;* orcid.org/0000-0002-0532-996X

Complete contact information is available at: https://pubs.acs.org/10.1021/acsinfecdis.2c00478

Author Contributions

Conceptualization: A.E.W., M.N.W., F.A.H., I.L., J.M.W., V.K., and L.K.T.; methodology: A.E.W., M.N.W., F.A.H., I.L., K.R.L., V.K., and L.K.T.; investigation: A.E.W., D.S., M.N.W., F.A.H., V.K., I.L., and K.R.L.; visualization: A.E.W., F.A.H., M.N.W., and V.K.; supervision: J.M.W. and L.K.T.; writing—original draft: A.E.W.; and writing—review and editing: all authors.

Funding

National Institutes of Health grant F30 HD101348 (A.E.W.); National Institutes of Health grant R01 AI30557 (L.K.T.); National Institutes of Health grant R01 GM138887 (F.A.H. and M.N.W.); National Institutes of Health grant R35 GM134949 (I.L.); National Institutes of Health grant R01 GM120351 (K.R.L.); National Institutes of Health grant T32 GM080186 (A.E.W.); National Institutes of Health grant T32 GM007267 (A.E.W.); Volkswagen Foundation Grant 93091 (I.L.); and William Wheless III professorship (M.N.W.).

Notes

The authors declare no competing financial interest.
All data, code, and materials used in the analyses available upon request.

■ ACKNOWLEDGMENTS

We thank Drs. Barbie Ganser-Pornillos and Kelly Dryden for expert help with the collection of the cryo-EM data acquired at the Molecular Electron Microscopy Core at the University of Virginia, which is supported in part by NIH grant U24 GM116790. Additionally, we thank the lab of Dr. Cliff Stains for assistance with the collection of FLIM spectra.

■ REFERENCES

(1) Rosa, A.; Chande, A.; Ziglio, S.; De Sanctis, V.; Bertorelli, R.; Goh, S. L.; McCauley, S. M.; Nowosielska, A.; Antonarakis, S. E.; Luban, J.; Santoni, F. A.; Pizzato, M. HIV-1 Nef Promotes Infection by Excluding SERINC5 from Virion Incorporation. *Nature* **2015**, *526*, 212−217.

(2) Usami, Y.; Wu, Y.; Göttlinger, H. G. SERINC3 and SERINC5 Restrict HIV-1 Infectivity and Are Counteracted by Nef. *Nature* **2015**, *526*, 218−223.

(3) Ward, A. E.; Kiessling, V.; Pornillos, O.; White, J. M.; Ganser-Pornillos, B. K.; Tamm, L. K. HIV-Cell Membrane Fusion Intermediates Are Restricted by Serincs as Revealed by Cryo Electron and TIRF Microscopy. *J. Biol. Chem.* **2020**, *295*, 15183−15195.

(4) Sood, C.; Marin, M.; Chande, A.; Pizzato, M.; Melikyan, G. B. SERINC5 Protein Inhibits HIV-1 Fusion Pore Formation by Promoting Functional Inactivation of Envelope Glycoproteins. *J. Biol. Chem.* **2017**, *292*, 6014−6026.

(5) Schulte, B.; Selyutina, A.; Opp, S.; Herschhorn, A.; Sodroski, J. G.; Pizzato, M.; Diaz-Griffero, F. Localization to Detergent-Resistant Membranes and HIV-1 Core Entry Inhibition Correlate with HIV-1 Restriction by SERINC5. *Virology* **2018**, *515*, 52−65.

(6) Staropoli, I.; Dufloo, J.; Ducher, A.; Commere, P.-H.; Sartori-Rupp, A.; Novault, S.; Bruel, T.; Lorin, V.; Mouquet, H.; Schwartz, O.; Casartelli, N. Flow Cytometry Analysis of HIV-1 Env Conformations at the Surface of Infected Cells and Virions: Role of Nef, CD4, and SERINC5. *J. Virol.* **2020**, *94*, No. e01783-19.

(7) Beitari, S.; Ding, S.; Pan, Q.; Finzi, A.; Liang, C. Effect of HIV-1 Env on SERINC5 Antagonism. *J. Virol.* **2017**, *91*, No. e02214-16.
(8) Chen, Y.-C.; Sood, C.; Marin, M.; Aaron, J.; Gratton, E.; Salaita, K.; Melikyan, G. B. Super-Resolution Fluorescence Imaging Reveals That Serine Incorporator Protein 5 Inhibits Human Immunodeficiency Virus Fusion by Disrupting Envelope Glycoprotein Clusters. *ACS Nano* **2020**, *14*, 10929.
(9) Harrison, S. C. Viral Membrane Fusion. *Virology* **2015**, *479-480*, 498−507.
(10) White, J. M.; Whittaker, G. R. Fusion of Enveloped Viruses in Endosomes. *Traffic* **2016**, *17*, 593−614.
(11) Kozlov, M. M.; Chernomordik, L. V. Membrane Tension and Membrane Fusion. *Curr. Opin. Struct. Biol.* **2015**, *33*, 61−67.
(12) Gracià, R. S.; Bezlyepkina, N.; Knorr, R. L.; Lipowsky, R.; Dimova, R. Effect of Cholesterol on the Rigidity of Saturated and Unsaturated Membranes: Fluctuation and Electrodeformation Analysis of Giant Vesicles. *Soft Matter* **2010**, *6*, 1472−1482.
(13) Chernomordik, L. V.; Kozlov, M. M. Mechanics of Membrane Fusion. *Nat. Struct. Mol. Biol.* **2008**, *15*, 675−683.
(14) Domanska, M. K.; Wrona, D.; Kasson, P. M. Multiphasic Effects of Cholesterol on Influenza Fusion Kinetics Reflect Multiple Mechanistic Roles. *Biophys. J.* **2013**, *105*, 1383−1387.
(15) Zawada, K. E.; Wrona, D.; Rawle, R. J.; Kasson, P. M. Influenza Viral Membrane Fusion Is Sensitive to Sterol Concentration but Surprisingly Robust to Sterol Chemical Identity. *Sci. Rep.* **2016**, *6*, 29842.
(16) Wudiri, G. A.; Schneider, S. M.; Nicola, A. V. Herpes Simplex Virus 1 Envelope Cholesterol Facilitates Membrane Fusion. *Front. Microbiol.* **2017**, *8*, 2383.
(17) Kasson, P. M.; Pande, V. S. Control of Membrane Fusion Mechanism by Lipid Composition: Predictions from Ensemble Molecular Dynamics. *PLoS Comput. Biol.* **2007**, *3*, No. e220.
(18) Yang, S.-T.; Kreutzberger, A. J.; Lee, J.; Kiessling, V.; Tamm, L. K. The Role of Cholesterol in Membrane Fusion. *Chem. Phys. Lipids* **2016**, *199*, 136−143.
(19) Chlanda, P.; Mekhedov, E.; Waters, H.; Schwartz, C. L.; Fischer, E. R.; Ryham, R. J.; Cohen, F. S.; Blank, P. S.; Zimmerberg, J. The Hemifusion Structure Induced by Influenza Virus Haemagglutinin Is Determined by Physical Properties of the Target Membranes. *Nat. Microbiol.* **2016**, *1*, 16050.
(20) Yang, S.-T.; Kreutzberger, A. J. B.; Kiessling, V.; Ganser-Pornillos, B. K.; White, J. M.; Tamm, L. K. HIV Virions Sense Plasma Membrane Heterogeneity for Cell Entry. *Sci. Adv.* **2017**, *3*, No. e1700338.
(21) Sun, X.; Whittaker, G. R. Role for Influenza Virus Envelope Cholesterol in Virus Entry and Infection. *J. Virol.* **2003**, *77*, 12543−12551.
(22) Haldar, S.; Mekhedov, E.; McCormick, C. D.; Blank, P. S.; Zimmerberg, J. Lipid-Dependence of Target Membrane Stability during Influenza Viral Fusion. *J. Cell Sci.* **2018**, *132*, No. jcs218321.
(23) Biswas, S.; Yin, S. R.; Blank, P. S.; Zimmerberg, J. Cholesterol Promotes Hemifusion and Pore Widening in Membrane Fusion Induced by Influenza Hemagglutinin. *J. Gen. Physiol.* **2008**, *131*, 503−513.
(24) Lee, J.; Kreutzberger, A. J. B.; Odongo, L.; Nelson, E. A.; Nyenhuis, D. A.; Kiessling, V.; Liang, B.; Cafiso, D. S.; White, J. M.; Tamm, L. K. Ebola Virus Glycoprotein Interacts with Cholesterol to Enhance Membrane Fusion and Cell Entry. *Nat. Struct. Mol. Biol.* **2021**, *28*, 181−189.
(25) Trautz, B.; Wiedemann, H.; Lüchtenborg, C.; Pierini, V.; Kranich, J.; Glass, B.; Kräusslich, H.-G.; Brocker, T.; Pizzato, M.; Ruggieri, A.; Brügger, B.; Fackler, O. T. The Host-Cell Restriction Factor SERINC5 Restricts HIV-1 Infectivity without Altering the Lipid Composition and Organization of Viral Particles. *J. Biol. Chem.* **2017**, *292*, 13702−13713.
(26) Huarte, N.; Carravilla, P.; Cruz, A.; Lorizate, M.; Nieto-Garai, J.; Kräusslich, H.-G. G.; Jesús, P.-G.; Jose, R.-I.; Nieva, J. L. L. Functional Organization of the HIV Lipid Envelope. *Sci. Rep.* **2016**, *6*, 34190.
(27) Brügger, B.; Glass, B.; Haberkant, P.; Leibrecht, I.; Wieland, F. T.; Kräusslich, H. G. The HIV Lipidome: A Raft with an Unusual Composition. *Proc. Natl. Acad. Sci. U. S. A.* **2006**, *103*, 2641−2646.
(28) Yang, S.-T.; Kiessling, V.; Simmons, J. A.; White, J. M.; Tamm, L. K. HIV Gp41−Mediated Membrane Fusion Occurs at Edges of Cholesterol-Rich Lipid Domains. *Nat. Chem. Biol.* **2015**, *11*, 424−431.
(29) Feigenson, G. W. Phase Behavior of Lipid Mixtures. In *Nature Chemical Biology*; Nature Publishing Group, 2006, pp 560−563, DOI: 10.1038/nchembio1106-560.
(30) Levental, I.; Levental, K. R.; Heberle, F. A. Lipid Rafts: Controversies Resolved, Mysteries Remain. *Trends Cell Biol.* **2020**, *30*, 341.
(31) Ashdown, G. W.; Owen, D. M. Imaging Membrane Order Using Environmentally Sensitive Fluorophores. *Methods Mol. Biol.* **2015**, *1232*, 115−122.
(32) Colom, A.; Derivery, E.; Soleimanpour, S.; Tomba, C.; Molin, M. D.; Sakai, N.; González-Gaitán, M.; Matile, S.; Roux, A. A Fluorescent Membrane Tension Probe. *Nat. Chem.* **2018**, *10*, 1118−1125.
(33) Niko, Y.; Didier, P.; Mely, Y.; Konishi, G.; Klymchenko, A. S. Bright and Photostable Push-Pull Pyrene Dye Visualizes Lipid Order Variation between Plasma and Intracellular Membranes. *Sci. Rep.* **2016**, *6*, 18870.
(34) Heberle, F. A.; Doktorova, M.; Scott, H. L.; Skinkle, A. D.; Waxham, M. N.; Levental, I. Direct Label-Free Imaging of Nanodomains in Biomimetic and Biological Membranes by Cryogenic Electron Microscopy. *Proc. Natl. Acad. Sci. U. S. A.* **2020**, *117*, 19943−19952.
(35) Cornell, C. E.; Mileant, A.; Thakkar, N.; Lee, K. K.; Keller, S. L. Direct Imaging of Liquid Domains in Membranes by Cryo-Electron Tomography. *Proc. Natl. Acad. Sci. U. S. A.* **2020**, *117*, 19713−19719.
(36) Lorent, J. H.; Levental, K. R.; Ganesan, L.; Rivera-Longsworth, G.; Sezgin, E.; Doktorova, M.; Lyman, E.; Levental, I. Plasma Membranes Are Asymmetric in Lipid Unsaturation, Packing and Protein Shape. *Nat. Chem. Biol.* **2020**, *16*, 644−652.
(37) Callahan, M. K.; Popernack, P. M.; Tsutsui, S.; Truong, L.; Schlegel, R. A.; Henderson, A. J. Phosphatidylserine on HIV Envelope Is a Cofactor for Infection of Monocytic Cells. *J. Immunol.* **2003**, *170*, 4840−4845.
(38) Amara, A.; Mercer, J. Viral Apoptotic Mimicry. *Nat. Rev. Microbiol.* **2015**, *13*, 461−469.
(39) Chua, B. A.; Ngo, J. A.; Situ, K.; Morizono, K. Roles of Phosphatidylserine Exposed on the Viral Envelope and Cell Membrane in HIV-1 Replication. *Cell Commun. Signaling* **2019**, *17*, 132.
(40) Dal Molin, M.; Verolet, Q.; Colom, A.; Letrun, R.; Derivery, E.; Gonzalez-Gaitan, M.; Vauthey, E.; Roux, A.; Sakai, N.; Matile, S. Fluorescent Flippers for Mechanosensitive Membrane Probes. *J. Am. Chem. Soc.* **2015**, *137*, 568−571.
(41) Licari, G.; Strakova, K.; Matile, S.; Tajkhorshid, E. Twisting and Tilting of a Mechanosensitive Molecular Probe Detects Order in Membranes. *Chem. Sci.* **2020**, *11*, 5637−5649.
(42) Goujon, A.; Colom, A.; Straková, K.; Mercier, V.; Mahecic, D.; Manley, S.; Sakai, N.; Roux, A.; Matile, S. Mechanosensitive Fluorescent Probes to Image Membrane Tension in Mitochondria, Endoplasmic Reticulum, and Lysosomes. *J. Am. Chem. Soc.* **2019**, *141*, 3380−3384.
(43) De Almeida, R. F. M.; Fedorov, A.; Prieto, M. Sphingomyelin/Phosphatidylcholine/Cholesterol Phase Diagram: Boundaries and Composition of Lipid Rafts. *Biophys. J.* **2003**, *85*, 2406−2416.
(44) Ionova, I. V.; Livshits, V. A.; Marsh, D. Phase Diagram of Ternary Cholesterol/Palmitoylsphingomyelin/ Palmitoyloleoyl-Phosphatidylcholine Mixtures: Spin-Label EPR Study of Lipid-Raft Formation. *Biophys. J.* **2012**, *102*, 1856−1865.
(45) Lin, C. M.; Li, C. S.; Sheng, Y. J.; Wu, D. T.; Tsao, H. K. Size-Dependent Properties of Small Unilamellar Vesicles Formed by Model Lipids. *Langmuir* **2012**, *28*, 689−700.

(46) Lipowsky, R. Remodeling of Membrane Shape and Topology by Curvature Elasticity and Membrane Tension. In *Advanced Biology*; John Wiley and Sons Inc, 2022, DOI: 10.1002/adbi.202101020.
(47) Fan, Z. A.; Tsang, K. Y.; Chen, S. H.; Chen, Y. F. Revisit the Correlation between the Elastic Mechanics and Fusion of Lipid Membranes. *Sci. Rep.* **2016**, *6*, 31470.
(48) Gupta, A.; Kallianpur, M.; Roy, D. S.; Engberg, O.; Chakrabarty, H.; Huster, D.; Maiti, S. Different Membrane Order Measurement Techniques Are Not Mutually Consistent. *Biophys. J.* **2022**, *S0006-3495*, No. 00689-0.
(49) Raghunath, G.; Chen, Y.-C.; Marin, M.; Wu, H.; Melikyan, G. B. SERINC5-Mediated Restriction of HIV-1 Infectivity Correlates with Resistance to Cholesterol Extraction but Not with Lipid Order of Viral Membrane. *Viruses* **2022**, *14*, 1636.
(50) M'Baye, G.; Mély, Y.; Duportail, G.; Klymchenko, A. S. Liquid Ordered and Gel Phases of Lipid Bilayers: Fluorescent Probes Reveal Close Fluidity but Different Hydration. *Biophys. J.* **2008**, *95*, 1217−1225.
(51) Kreutzberger, A. J. B.; Kiessling, V.; Liang, B.; Yang, S.-T.; Castle, J. D.; Tamm, L. K. Asymmetric Phosphatidylethanolamine Distribution Controls Fusion Pore Lifetime and Probability. *Biophys. J.* **2017**, *113*, 1912−1915.
(52) Yang, S.-T.; Kiessling, V.; Tamm, L. K. Line Tension at Lipid Phase Boundaries as Driving Force for HIV Fusion Peptide-Mediated Fusion. *Nat. Commun.* **2016**, *7*, 11401.
(53) Lorizate, M.; Brügger, B.; Akiyama, H.; Glass, B.; Müller, B.; Anderluh, G.; Wieland, F. T.; Kräusslich, H. G. Probing HIV-1 Membrane Liquid Order by Laurdan Staining Reveals Producer Cell-Dependent Differences. *J. Biol. Chem.* **2009**, *284*, 22238−22247.
(54) Eells, R.; Barros, M.; Scott, K. M.; Karageorgos, I.; Heinrich, F.; Lösche, M. Structural Characterization of Membrane-Bound Human Immunodeficiency Virus-1 Gag Matrix with Neutron Reflectometry. *Biointerphases* **2017**, *12*, No. 02D408.
(55) Qu, K.; Ke, Z.; Zila, V.; Anders-Össwein, M.; Glass, B.; Mücksch, F.; Müller, R.; Schultz, C.; Müller, B.; Kräusslich, H.-G.; Briggs, J. A. G. Maturation of the Matrix and Viral Membrane of HIV-1. *Science* **2021**, *373*, 700−704.
(56) O'Neil, L.; Andenoro, K.; Pagano, I.; Carroll, L.; Langer, L.; Dell, Z.; Perera, D.; Treece, B. W.; Heinrich, F.; Lösche, M.; Nagle, J. F.; Tristram-Nagle, S. HIV-1 Matrix-31 Membrane Binding Peptide Interacts Differently with Membranes Containing PS vs. PI(4,5)P2. *Biochim. Biophys. Acta, Biomembr.* **2016**, *1858*, 3071−3081.
(57) Schwarzer, R.; Levental, I.; Gramatica, A.; Scolari, S.; Buschmann, V.; Veit, M.; Herrmann, A. The Cholesterol-Binding Motif of the HIV-1 Glycoprotein Gp41 Regulates Lateral Sorting and Oligomerization. *Cell. Microbiol.* **2014**, *16*, 1565−1581.
(58) Brandenberg, O. F.; Magnus, C.; Regoes, R. R.; Trkola, A. The HIV-1 Entry Process: A Stoichiometric View. *Trends Microbiol.* **2015**, 763.
(59) Leonhardt, S. A.; Purdy, M. D.; Grover, J. R.; Yang, Z.; Poulos, S.; McIntire, W. E.; Tatham, E. A.; Erramilli, S.; Nosol, K.; Lai, K. K.; Ding, S.; Lu, M.; Uchil, P. D.; Finzi, A.; Rein, A.; Kossiakoff, A. A.; Mothes, W.; Yeager, M. CryoEM Structures of the Human HIV-1 Restriction Factor SERINC3 and Function as a Lipid Transporter. *bioRxiv* **2022**, DOI: 10.1101/2022.07.06.498924.
(60) Kirschman, J.; Marin, M.; Chen, Y.-C.; Chen, J.; Herschhorn, A.; III, A.; Melikyan, G. B. SERINC5 Restricts HIV-1 Infectivity by Promoting Conformational Changes and Accelerating Functional Inactivation of Env. *Viruses* **2022**, *14*, 1388.
(61) Hollingsworth, L. R.; Lemkul, J. A.; Bevan, D. R.; Brown, A. M. HIV-1 Env Gp41 Transmembrane Domain Dynamics Are Modulated by Lipid, Water, and Ion Interactions. *Biophys. J.* **2018**, *115*, 84−94.
(62) Steinkühler, J.; Sezgin, E.; Urbančič, I.; Eggeling, C.; Dimova, R. Mechanical Properties of Plasma Membrane Vesicles Correlate with Lipid Order, Viscosity and Cell Density. *Commun. Biol.* **2019**, *2*, 337.
(63) Usery, R. D.; Enoki, T. A.; Wickramasinghe, S. P.; Weiner, M. D.; Tsai, W. C.; Kim, M. B.; Wang, S.; Torng, T. L.; Ackerman, D. G.; Heberle, F. A.; Katsaras, J.; Feigenson, G. W. Line Tension Controls Liquid-Disordered + Liquid-Ordered Domain Size Transition in Lipid Bilayers. *Biophys. J.* **2017**, *112*, 1431−1443.
(64) Kliesch, T. T.; Dietz, J.; Turco, L.; Halder, P.; Polo, E.; Tarantola, M.; Jahn, R.; Janshoff, A. Membrane Tension Increases Fusion Efficiency of Model Membranes in the Presence of SNAREs. *Sci. Rep.* **2017**, *7*, 12070.
(65) Shillcock, J. C.; Lipowsky, R. Tension-Induced Fusion of Bilayer Membranes and Vesicles. *Nat. Mater.* **2005**, *4*, 225−228.
(66) Staykova, M.; Holmes, D. P.; Read, C.; Stone, H. A. Mechanics of Surface Area Regulation in Cells Examined with Confined Lipid Membranes. *Proc. Natl. Acad. Sci. U. S. A.* **2011**, *108*, 9084−9088.
(67) Ryham, R. J.; Klotz, T. S.; Yao, L.; Cohen, F. S. Calculating Transition Energy Barriers and Characterizing Activation States for Steps of Fusion. *Biophys. J.* **2016**, *110*, 1110−1124.
(68) Siegel, D. P. The Gaussian Curvature Elastic Energy of Intermediates in Membrane Fusion. *Biophys. J.* **2008**, *95*, 5200−5215.
(69) Pye, V. E.; Rosa, A.; Bertelli, C.; Struwe, W. B.; Maslen, S. L.; Corey, R.; Liko, I.; Hassall, M.; Mattiuzzo, G.; Ballandras-Colas, A.; Nans, A.; Takeuchi, Y.; Stansfeld, P. J.; Skehel, J. M.; Robinson, C. V.; Pizzato, M.; Cherepanov, P. A Bipartite Structural Organization Defines the SERINC Family of HIV-1 Restriction Factors. *Nat. Struct. Mol. Biol.* **2020**, *27*, 78−83.
(70) Churchward, M. A.; Rogasevskaia, T.; Brandman, D. M.; Khosravani, H.; Nava, P.; Atkinson, J. K.; Coorssen, J. R. Specific Lipids Supply Critical Negative Spontaneous Curvature-an Essential Component of Native Ca2+−Triggered Membrane Fusion. *Biophys. J.* **2008**, *94*, 3976−3986.
(71) Chernomordik, L. V.; Kozlov, M. M. Membrane Hemifusion: Crossing a Chasm in Two Leaps. *Cell* **2005**, *123*, 375−382.
(72) Padilla-Parra, S.; Marin, M.; Gahlaut, N.; Suter, R.; Kondo, N.; Melikyan, G. B. *Fusion of Mature HIV-1 Particles Leads to Complete Release of a Gag-GFP-Based Content Marker and Raises the Intraviral PH. PLoS One* 2013, *8* (8), e71002, DOI: 10.1371/journal.-pone.0071002.
(73) Wagner, M. L.; Tamm, L. K. Tethered Polymer-Supported Planar Lipid Bilayers for Reconstitution of Integral Membrane Proteins: Silane-Polyethyleneglycol-Lipid as a Cushion and Covalent Linker. *Biophys. J.* **2000**, *79*, 1400−1414.
(74) Cheng-Mayer, C.; Liu, R.; Landau, N. R.; Stamatatos, L. Macrophage Tropism of Human Immunodeficiency Virus Type 1 and Utilization of the CC-CKR5 Coreceptor. *J. Virol.* **1997**, *71*, 1657−1661.
(75) Stamatatos, L.; Lim, M.; Cheng-Mayer, C. Generation and Structural Analysis of Soluble Oligomeric Gp140 Envelope Proteins Derived from Neutralization-Resistant and Neutralization-Susceptible Primary HIV Type 1 Isolates. *AIDS Res. Hum. Retroviruses* **2000**, *16*, 981.
(76) Stamatatos, L.; Wiskerchen, M.; Cheng-Mayer, C. Effect of Major Deletions in the V1 and V2 Loops of a Macrophage-Tropic HIV Type 1 Isolate on Viral Envelope Structure, Cell Entry, and Replication. *AIDS Res. Hum. Retroviruses* **1998**, *14*, 1129.
(77) Hulseberg, C. E.; Fénéant, L.; Wijs, K. M. S.; Kessler, N. P.; Nelson, E. A.; Shoemaker, C. J.; Schmaljohn, C. S.; Polyak, S. J.; White, J. M. Arbidol and Other Low-Molecular-Weight Drugs That Inhibit Lassa and Ebola Viruses. *J. Virol.* **2019**, *93*, No. e02185-18.
(78) Wehrly, K.; Chesebro, B. P24 Antigen Capture Assay for Quantification of Human Immunodeficiency Virus Using Readily Available Inexpensive Reagents. *Methods* **1997**, *12*, 288−293.
(79) Toohey, K.; Wehrly, K.; Nishio, J.; Perryman, S.; Chesebro, B. Human Immunodeficiency Virus Envelope V1 and V2 Regions Influence Replication Efficiency in Macrophages by Affecting Virus Spread. *Virology* **1995**, *213*, 70−79.
(80) Diehl, W. E.; Guney, M. H.; Kyawe, P. P.; White, J. M.; Pizzato, M.; Luban, J. Influence of Different Glycoproteins and of the Virion Core on SERINC5 Antiviral Activity. *Viruses* **2021**, *13*, 1279.
(81) Sezgin, E.; Kaiser, H.-J.; Baumgart, T.; Schwille, P.; Simons, K.; Levental, I. Elucidating Membrane Structure and Protein Behavior Using Giant Plasma Membrane Vesicles. *Nat. Protoc.* **2012**, *7*, 1042−1051.

(82) Kalb, E.; Frey, S.; Tamm, L. K. Formation of Supported Planar Bilayers by Fusion of Vesicles to Supported Phospholipid Monolayers. *Biochim. Biophys. Acta, Biomembr.* **1992**, *1103*, 307−316.
(83) Zheng, S. Q.; Palovcak, E.; Armache, J.-P.; Verba, K. A.; Cheng, Y.; Agard, D. A. MotionCor2: Anisotropic Correction of Beam-Induced Motion for Improved Cryo-Electron Microscopy. *Nat. Methods* **2017**, *14*, 331−332.
(84) Kuzmin, P. I.; Akimov, S. A.; Chizmadzhev, Y. A.; Zimmerberg, J.; Cohen, F. S. Line Tension and Interaction Energies of Membrane Rafts Calculated from Lipid Splay and Tilt. *Biophys. J.* **2005**, *88*, 1120−1133.

https://doi.org/10.1021/acsinfecdis.2c00478
ACS Infect. Dis. 2023, 9, 773−784